ILETA International Information and Engineering Technology Association

Mathematical Modelling of Engineering Problems

Vol. 12, No. 9, September, 2025, pp. 2981-2992

Journal homepage: http://iieta.org/journals/mmep

Thermo-Mechanical Response of Reinforced Geopolymer Hollow Beams Containing Steel Fibers



Gonol Ali Mardan¹, Mazin Burhan Al-Deen Abdul-Rahman¹, Arjan Fakhrulddin Abdullah², Zainab Al-Khafaji^{3,4*}

- ¹ Department of Civil Engineering, Structure Engineering, Faculty of Engineering, University of Tikrit, Tikrit 34001, Iraq
- ² Department of Architecture and Construction Engineering, Technical Engineering College of Kirkuk, Northern Technical University, Kirkuk 36001, Iraq
- ³ Department of Civil Engineering, Faculty of Engineering and Built Environment, Universiti Kebangsaan Malaysia, UKM Bangi, Bangi 43600, Malaysia
- ⁴ Department of Cooling and Air Conditioning Engineering, Imam Ja'afar Al-Sadiq University, Qahira, Baghdad 10053, Iraq

Corresponding Author Email: P123005@siswa.ukm.edu.my

Copyright: ©2025 The authors. This article is published by IIETA and is licensed under the CC BY 4.0 license (http://creativecommons.org/licenses/by/4.0/).

https://doi.org/10.18280/mmep.120903

Received: 9 July 2025 Revised: 7 September 2025 Accepted: 12 September 2025 Available online: 30 September 2025

Kevwords:

geopolymer concrete (GPC), steel fibers, elevated temperatures, residual strength, flexural behavior, hollow beam

ABSTRACT

The increasing demand for sustainable and fire-resilient infrastructure has accelerated research on geopolymer concrete (GPC) as an eco-friendly alternative to ordinary Portland cement (OPC). This study presents the first full-scale experimental investigation of reinforced GPC beams incorporating both hollow cross-sections and steel fibers, evaluated under elevated temperatures up to 750°C. Twenty beams were fabricated using fly ash-Ground Granulated Blast Furnace Slag (GGBS) binders activated by alkaline solutions, with steel fibers added at 0-1% volume fractions. Fullscale flexural testing was conducted at ambient, 250°C, 500°C, and 750°C to assess load-deflection behavior, ductility, stiffness, toughness, and residual capacity. Results revealed that solid beams consistently outperformed hollow beams, achieving up to 18% higher load capacity, 24% greater stiffness, and 47% superior residual strength at 750°C. Steel fibers enhanced crack-bridging, toughness, and thermal stability, with 1% fiber content providing optimal fire resistance. Hollow beams, while advantageous for strength-to-weight efficiency, failed completely at 750°C due to accelerated thermal gradients and spalling. The combined influence of hollow geometry and fiber reinforcement under fire has not been systematically addressed in previous studies, positioning this work at the intersection of sustainability and fire safety. Beyond structural performance, the replacement of OPC with FA-GGBS reduced embodied CO₂ emissions by an estimated ~350 kg per m³ of concrete, highlighting the environmental benefits of GPC in high-risk fire applications.

1. INTRODUCTION

The increasing demand for sustainable and highperformance construction materials has led to significant interest in geopolymers—aluminosilicate-based binders synthesized through the activation of industrial by-products, such as fly ash (FA) and slag. These materials offer notable environmental advantages over traditional Portland cement, including reduced carbon emissions and enhanced resistance to fire and chemical attacks [1-5]. Despite their benefits, geopolymers are inherently brittle, limiting their structural applications. Incorporating fibers into the geopolymer matrix has emerged as an effective strategy to enhance mechanical properties. Steel fibers, in particular, have demonstrated significant improvements in flexural strength, toughness, and resistance to cracking. For instance, adding 3% steel fibers by weight to fly ash-based geopolymer composites increased the flexural strength from 4 to 35 MPa and the compressive strength from 31 to 55 MPa over a 56-day period [6].

Hollow beam structures are widely utilized in engineering due to their favorable strength-to-weight ratios. However, their performance under combined thermal and mechanical loads, especially when reinforced with steel fibers, remains underexplored [7]. Understanding the thermo-mechanical behavior of such reinforced hollow beams is crucial for their application in environments subjected to high temperatures and mechanical stresses, such as in aerospace and industrial settings. This research aims to investigate the thermo-mechanical response of reinforced geopolymer hollow beams containing steel fibers. By examining how steel fiber reinforcement influences the structural integrity and thermal stability of these beams, the study seeks to provide insights into their potential applications in demanding environments [8, 9].

Madheswaran et al. [10] explored the strength development of concrete using sodium hydroxide (NaOH) solutions with varying molarities. In this study, 150 mm cubes and 150 mm \times 300 mm cylinders were cast using Na₂SiO₃ and NaOH

solutions with varying molarities (3 M, 5 M, and 7 M) as alkaline activators and cured under ambient conditions, with an alkaline activator to GGBS ratio of 0.65. The 7-day compressive strengths recorded were 44, 46, and 48 N/mm² for the 3 M, 5 M, and 7 M solutions, respectively. By the 28th day, the compressive strengths had increased to 47, 54, and 60 N/mm², respectively. The specimen activated with 5 M NaOH achieved a splitting tensile strength of 5.3 N/mm² approximately 10% of its compressive strength. The findings indicated that both compressive and splitting tensile strengths increased with higher molarity of the activating solution. When compared to ordinary Portland cement (OPC) concrete, which exhibited splitting tensile strength of 4.5 N/mm² and compressive strengths of 19 N/mm² and 45 N/mm² at 7 and 28 days, respectively, the geopolymer concrete demonstrated significantly improved performance.

Arun et al. [11] investigated the mechanical behavior of geopolymer concrete (GPC), specifically focusing on its tensile, compressive, and flexural strengths. Their study examined the combined effect of FA and Ground Granulated Blast Furnace Slag (GGBFS) [12, 13], where FA was replaced with GGBFS at varying proportions of 0%, 30%, 50%, and 70% by mass, using a trial-and-error approach. The total binder content was maintained at 400 kg/m³, and the alkali activator-to-binder ratio was fixed at 0.47 by mass. The findings revealed that higher GGBFS content and increased NaOH molarity significantly enhanced the mechanical performance of GPC. Notably, the compressive strength reached 49 MPa after 56 days of curing. Furthermore, replacing FA with GGBFS resulted in a marked performance improvement, with up to a 70% replacement showing substantial gains. Notably, this included a 7.40% increase in tensile strength and a 12.64% rise in flexural strength at 56

Self-compacting geopolymer concrete (SCGC) has gained attention as a sustainable alternative to traditional concrete. Its performance is largely influenced by the type and proportion of aluminosilicate binders, primarily FA and GGBFS. Studies have examined SCGC mixes with varying FA-GGBFS ratios (0–100%, 50–50%, and 100–0%) using a constant binder content (500 kg/m³) and alkali-to-binder ratio (0.5), activated by sodium hydroxide and sodium silicate solutions [14].

The mechanical and fresh properties of SCGC vary with curing conditions. Heat curing at 110°C improves early strength, especially in FA-rich mixes, while GGBFS enhances long-term strength under ambient conditions. However, high GGBFS content reduces workability. Notably, the 50% FA-50% GGBFS blend offers an optimal balance of strength, workability, and environmental benefit, making it a promising eco-friendly SCGC mix.

Bellum et al. [15] investigated the mechanical performance of GPC produced using FA and GGBFS, with sodium hydroxide (NaOH) solutions of varying molarities ranging from 6 M to 14 M. Their research revealed that the GPC samples—composed of inorganic binders (FA and GGBFS)—were subjected to initial oven curing at 70°C for 24 hours, followed by natural sun curing for durations of 3, 7, 14, and 28 days. Under these curing conditions, the compressive strength peaked at 34.15 MPa after the initial 70°C heat treatment and subsequent 28 days of sun exposure. When using a 14 M NaOH solution and following the same curing protocol, the maximum observed splitting tensile strength was 3.87 MPa. Similarly, the highest recorded flexural strength reached 11.02 MPa. Furthermore, increasing the NaOH molarity from 8 M to

14 M led to notable improvements in mechanical properties: compressive strength increased by 33%, tensile strength by 26%, and flexural strength by 42.5%.

Saavedra and de Gutiérrez [16] reported that geopolymer concrete composed of GGBFS and FA demonstrates superior performance at elevated temperatures, particularly at 1100°C when compared to conventional Portland cement-based concrete. Similarly, Behfarnia and Shahbaz [17] studied the impact of high temperatures on alkali-activated slag (AAS) concrete, focusing on mass loss and residual tensile strength after curing periods of 7, 28, and 90 days. The AAS concrete samples were exposed to temperatures of 20, 200, 400, 600, and 800°C. For comparison, specimens made with ordinary Portland cement were also tested under the same conditions. The results revealed that AAS concrete retained significantly higher tensile strength than traditional concrete when subjected to elevated temperatures.

GPC is a promising, eco-friendly alternative to ordinary OPC, offering excellent mechanical properties and fire resistance. A key challenge addressed in recent studies is the spalling of concrete under high temperatures, especially in high-strength mixes. GPC has demonstrated the ability to retain up to 80% of its compressive strength after exposure to 800°C. Moreover, incorporating steel fibers improves thermal performance, increasing residual strength by up to 25% and significantly reducing spalling. These findings highlight GPC's resilience in fire-prone environments and the added value of fiber reinforcement [18].

Ahmed [19] explored the effects of elevated temperatures on FA-based GPC. The study assessed both the compressive strength and the indirect splitting tensile strength of GPC after exposure to high temperatures ranging from 200°C to 1000°C (specifically: 200°C, 300°C, 400°C, 500°C, 600°C, 700°C, 800°C, and 1000°C). The results indicated a progressive decline in compressive strength, with reductions of 8%, 13%, 15%, 17%, 24%, 38%, 46%, and 55%, respectively, corresponding to the increasing temperatures. Similarly, the indirect splitting tensile strength showed a consistent decrease of 12%, 17%, 22%, 28%, 36%, 44%, 53%, and 64% across the same temperature range.

Despite the growing body of literature on geopolymer concrete, several critical gaps persist in the field. First, most existing studies have focused on the compressive or tensile behavior of small-scale specimens, whereas element-level investigations of full-scale beams remain limited. Second, the fire performance of hollow GPC beams has not been adequately characterized, even though such members are widely employed for weight reduction in modern structures. Third, while steel fibers have been shown to improve toughness and crack resistance, their optimal dosage for enhancing fire endurance in GPC beams—particularly in configurations—has not been systematically evaluated. Finally, previous works have seldom established a clear connection between thermal exposure, structural degradation, and long-term residual capacity, leaving designers without reliable guidance for practical applications. This study directly addresses these gaps by experimentally evaluating the flexural behavior, ductility, toughness, and residual strength of solid and hollow GPC beams with varying steel fiber contents under elevated temperatures. The findings contribute essential insights for the development of fireresistant, sustainable design strategies for geopolymer-based structural members.

The motivation for this study is driven by the urgent need to

develop structural materials that can withstand fire hazards while simultaneously addressing the global demand for sustainable construction practices. Fire-induced failures in reinforced concrete structures continue to result in significant economic losses and safety concerns, with conventional OPCbased systems demonstrating severe spalling and rapid degradation under thermal loading. In parallel, the environmental burden associated with cement production necessitates the adoption of eco-efficient alternatives. Geopolymer concrete offers a viable solution by reducing CO₂ emissions by approximately 40-80% compared to OPC, while also exhibiting superior thermal stability. Moreover, hollow members are increasingly adopted in bridges, tunnels, and high-rise structures to reduce self-weight and improve material efficiency, yet their vulnerability under fire remains insufficiently understood. By investigating hollow GPC beams reinforced with steel fibers, this study addresses both the performance and sustainability requirements of fireexposed infrastructure, offering pathways toward safer and greener structural systems.

The novelty of this research lies in its systematic exploration of the combined effect of hollow cross-sectional geometry and steel fiber reinforcement on the thermomechanical performance of GPC beams exposed to elevated temperatures. While previous investigations have primarily concentrated on solid GPC members or on the influence of

fibers alone, the synergistic role of hollow sections and varying fiber contents under fire exposure has remained largely unexplored. This study is the first to present full-scale experimental evidence on the performance of hollow GPC beams reinforced with steel fibers when subjected to thermal loading up to 750°C. By integrating structural efficiency through hollow geometry, enhanced ductility through steel fiber reinforcement, and sustainability through the utilization of industrial by-products such as FA and GGBS, this work introduces a novel approach that bridges the gap between material sustainability and structural fire resilience.

2. METHODOLOGY

2.1 Material used

(a) Normal cement

In the preparation of GPC, Ordinary Portland Cement (Type I) was utilized as a reference binder for comparative analysis. It is a general-purpose cement suitable for most structural applications. Its chemical composition, including oxides such as CaO, SiO₂, and Al₂O₃, along with its physical properties, including fineness and specific gravity, are provided in Table 1 and Table 2. Standard procedures were used to test these properties and ensure material consistency.

Table 1. Physical properties

No.	Material	Specific Gravity	Specific Surface Area	Water Absorption (%)	Dry Loose Unit Weight (kg/m³)	Sulfate Amount (SO ₃) (%)	Material Passing Through the 0.075 mm Sieve
1	FA	2.44	521 m ² /kg	-	-	-	-
2	GGBS	2.57	$290 \text{ m}^2/\text{kg}$	-	-	-	-
3	Cement	2.58	$372 \text{ m}^2/\text{kg}$	-	-	-	-
4	Coarse aggregate	2.69	-	1.11	1625	0.088	-
5	Fine aggregate	2.44	-	1.22	1798	0.074	1.84

Table 2. Oxide composition of cement, FA, and GGBFS

Oxides Composition	FA	GGBFS	Cement
CaO	1.52	30.10	62.60
Al_2O_3	22.10	8.78	5.20
${ m SiO_2}$	62.22	35.40	21.5
Fe_2O_3	7.12	1.97	3.40
MgO	2.34	6.92	2.42
SO_3	0.15	0.41	2.44
Loss of Ignition (L.O.I)	1.55	0.80	1.81

(b) GGBFS

GGBFS, as defined by ACI - 233R-03 [20], is a non-metallic by-product formed during the production of molten pig iron in a blast furnace. It mainly consists of calcium silicates, aluminosilicates, and other basic oxides. The physical properties of GGBS used in this study are presented in Table 1 and Table 2.

(c) FA

As a cement alternative, Class F-FA conforming to the study [21] was used in this study. The FA, obtained from the EUROBUILD company, is a fine gray powder commonly used in construction materials. Its chemical and physical properties are presented in Tables 1 and 2.

(d) Sodium silicate (Na₂SIO₃) and Sodium hydroxide (NaOH) The alkaline activator used in geopolymer concrete is a combination of sodium silicate (Na_2SiO_3) and sodium hydroxide (NaOH). The effectiveness of sodium silicate depends on the silicate modulus (SiO_2/Na_2O), which is influenced by the proportion of SiO_2 to Na_2O , as well as the water content that affects the solution's viscosity and reactivity. Higher silicate ratios result in thicker, less reactive solutions, whereas lower ratios increase alkalinity and enhance reaction rates. Sodium hydroxide, supplied as 99% pure flakes, is dissolved in distilled water to achieve the required molarity, which is determined by the ratio of flakes to water. Due to the heat released during dissolution, the solution must be left to cool in open air for a minimum of two hours before use.

(e) Superplasticizer

In this study, Sika® ViscoCrete®-5930 was used as a superplasticizer (SP), also classified as a High-Range Water-Reducing (HRWR) admixture. This additive is chloride-free and complies with ASTM. It is commonly employed in concrete mixtures to enhance workability without increasing the water content, thereby improving overall performance.

(f) Aggregate properties and grading

In this study, river gravel with a nominal size of 12.5 mm was used as the coarse aggregate. It was tested according to the standard [22], and its sieve analysis is illustrated in Figure 1. The fine aggregate consisted of natural sand with a maximum particle size of 4.75 mm, meeting the grading

specifications [23]. The corresponding sieve analysis results are presented in Figure 2.

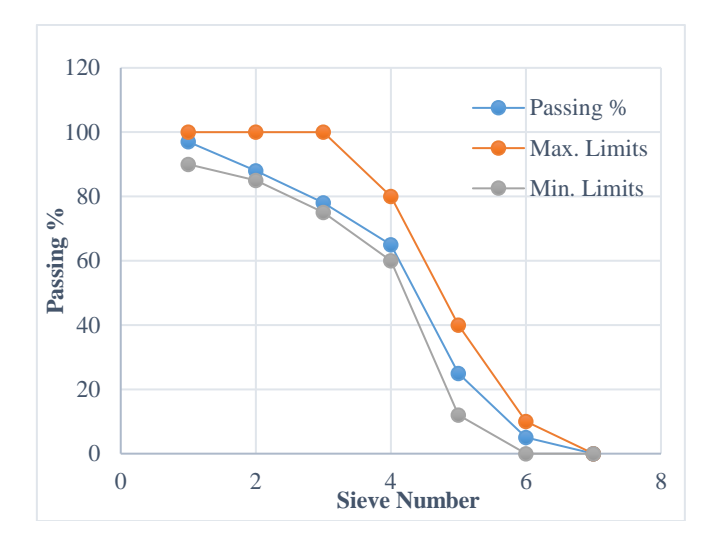


Figure 1. Particle size distribution of coarse aggregate

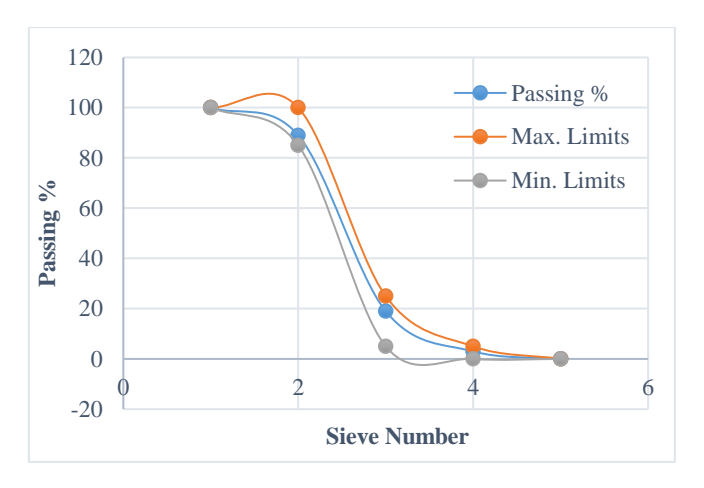


Figure 2. Particle size distribution of fine aggregate

(g) Steel fiber (SF)

In the current investigation, hooked-end steel fibers (SF) were incorporated into the GPC mix to enhance its tensile strength. The fibers were added at volume fractions of 0%, 0.5%, 0.75%, and 1% relative to the total volume of the GPC.

The steel fibers used were of a high-strength type, featuring an average diameter of approximately 0.55 mm, a length of 35 mm, and an aspect ratio of about 64. These fibers exhibited a maximum tensile strength of up to 1345 MPa.

(h) Steel reinforcement bars and plastic pipes

The beams were longitudinally reinforced with deformed steel bars of 12 mm and 8 mm diameters, while 8 mm deformed bars were used for the closed stirrups. To create hollow sections in the tension zone, 75 mm diameter plastic pipes were embedded. Being chemically inert, the plastic pipes do not interact with the reinforcement or geopolymer concrete constituents.

2.2 Mixture of designations

The mix proportions and preparation method for the geopolymer mortar were developed based on previous study [24]. At the initial stage of this research, several trial mixes were prepared and tested at 28 days of age. The results confirmed that the mix design shown in Table 3. provides suitable workability and strength for GPC. A constant alkaline activator-to-binder (AA/B) ratio of 0.4 was maintained, as this ratio has been shown to enhance both the microstructure and strength of the material. Additionally, a Na₂SiO₃ to NaOH ratio of 2.5 was adopted, in line with the study [24]. Various steel fiber volume fractions were used in the mixes of (0, 0.5, 0.75, 1) volume fraction percentages. The flow chart in Figure 3 explains the geopolymerization process.

Step 1/ Mixing coarse and fine aggregate for 1 minutes

Step 2/Adding the GGBFS, FA, and Cement with continuing mixing for 2 minutes

Step 3/ Adding the SF with continuing mixing for 2 minutes

Step 4/ Adding the alkaline solution with continuing mixing for

Step 5/ All components were mixed for additional 3 minutes (with SP) or until a homogeneous mixture to be obtained

Figure 3. Flow chart of mixing steps procedure of GPC

Table 3. Amount for GPC according to the specified mix design

Na ₂ SiO ₃ (kg)	NaOH (kg)	SS/SH Ratio	AA / Binder Ratio	FA (kg)	GGBS (kg)	Cement (kg)	Fine Agg. (kg)	Coarse Agg. (kg)	No.
129	21	2.5	0.4	168	210	42	690	1250	1

Table 4. Test matrix of the geopolymer concrete beams

Sample ID	Beam Details	Steel Fiber Ratio (%)	Degree of Temperature	Sample ID	Beam Details	Steel Fiber Ratio	Degree of Temperature
S1	S1-Am-0	0	Ambient	H33	H3-500-0.5	0.5	500°C
S2	S1-250-0	0	250°C	H34	H3-750-0.5	0.5	750°C
S 3	S1-500-0	0	500°C	H41	H4-Am-0.75	0.75	Ambient
S 4	S1-750-0	0	750°C	H42	H4-250-0.75	0.75	250°C
H21	H2-Am-0	0	Ambient	H43	H4-500-0.75	0.75	500°C
H22	H2-250-0	0	250°C	H44	H4-750-0.75	0.75	750°C
H23	H2-500-0	0	500°C	H51	H5-Am-1	1	Ambient
H24	H2-750-0	0	750°C	H52	H5-250-1	1	250°C
H31	H3-Am-0.5	0.5	Ambient	H53	H5-500-1	1	500°C
H32	H3-250-0.5	0.5	250°C	H54	H5-750-1	1	750°C

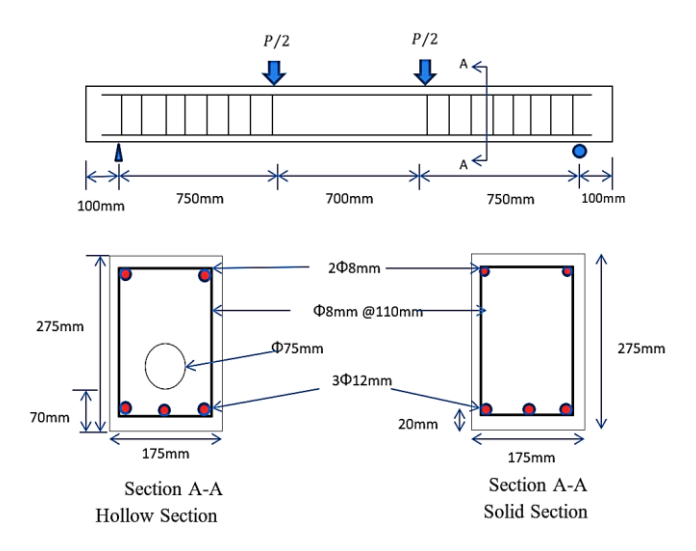


Figure 4. Dimensions and reinforcement details of reinforced beam



Figure 5. Casting and curing of specimens

(a) Beams specimens variables and designation

In this study, a total of twenty beams were tested, as detailed in Table 4. The beams were organized into five groups, each consisting of four specimens. The groups incorporated steel fibers at volumetric ratios of 0%, 0.5%, 0.75%, and 1%, respectively. All the groups featured hollow cross-sections except for the final group, which had a solid cross-section. Table 4 summarizes the tested beam specimens made of GPC, categorized by steel fiber content and exposure temperature. Each beam is identified by a symbol indicating its group, temperature condition, and steel fiber ratio. The steel fiber ratios used are 0%, 0.5%, 0.75%, and 1%. The beams were tested under four temperature conditions: ambient, 250°C, 500°C, and 750°C.

2.3 Casting of beam specimens

This study involved casting twenty full-scale GPC beams to evaluate their structural response and fire resistance. All beams had identical dimensions of 175×275 mm with a length of 2400 mm and a clear span of 2200 mm. Two types of sections were tested: solid and hollow, the latter containing a 75 mm circular void below the neutral axis. Reinforcement was designed per ACI 318-11 with an under-reinforced

arrangement, consisting of 3Ø12 mm tensile bars, 2Ø8 mm compression bars, and Ø8 mm stirrups at 110 mm spacing, with 20 mm cover as illustrated in Figure 4. Beam molds were fabricated from 3 mm thick steel plates using detachable parts for easy demolding as shown in Figure 5. Each mold had 75 mm round openings at both ends to secure plastic tubes for creating internal cavities. Before casting, molds were thoroughly cleaned and lubricated. Steel reinforcement was placed first, followed by the insertion of plastic pipes. The same mixing and casting procedure used for smaller specimens was applied. GPC was poured in three layers, each compacted with a needle vibrator to minimize air voids. After surface finishing with a steel trowel, the molds were removed after one day. To prevent moisture loss and shrinkage, beams were coated with a Sika curing compound and left to cure at normal room temp tell testing.

2.4 Test setup

A furnace was constructed to replicate building fire situations and assess structural damage under high temps. The setup included a steel frame for loading specimens both at room temp and during heating. The chamber measured about $1.47~\text{m}\times1.34~\text{m}\times2.80~\text{m}$ as shown in Figure 6 and consisted of three layers: an outer solid block, a ceramic fiber insulation (1260-degree centigrade rating), and inner fire bricks (1200-degree centigrade rating). The furnace had two chimneys for gas release and a 3 mm steel plate top insulated with ceramic wool. This system has been used to examine the flexural strength and fire resistance of beam specimens under load, as well as the performance of control samples (cubes, cylinders, prisms).

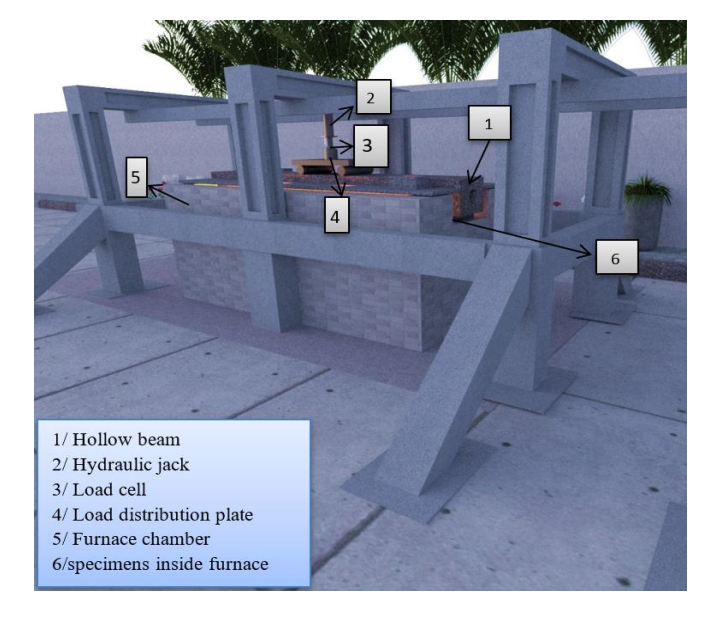


Figure 6. The detail of the loading frame

In this study, three sensor types were used: load cells, LVDTs, and type-K thermocouples. The thermocouples, connected to a digital recorder with ±1°C accuracy, tracked temp inside and outside the beams, while LVDTs linked to a data logger measured deflections. Three thermocouples were also positioned along the furnace chamber to control the temp for the specimen (cubes, cylinders, prisms) inside the furnace and to record temp distribution for the furnace and along the beam's length. Each beam was subjected to a sustained service load equal to 50% of its max capacity. During fire subject at

250, 500, and 750°C, data on mid-span deflection and temp were collected until either failure occurred or the two-hour test duration ended, after which the burners were shut down. After completing the fire subject stage, the furnace was switched off and left to cool naturally for about two hours to avoid sudden thermal shock. Once the temp dropped to a safe level, the specimens were carefully removed and inspected. Each sample was then subjected to residual testing, which involved recording visible cracks, spalling, and surface discoloration, followed by measuring its mechanical performance (compressive, flexural, or tensile strength) to evaluate the remaining capacity after fire subject.

3. RESULTS AND DISCUSSION

3.1 Materials properties testing results

(1) Compressive strength

The concrete compressive strengths were tested on both normal samples and residual samples after subject to high temps of 250, 500, and 750°C. Each "column" in the results represented the mean strength of three individual cubes. The concrete mix was consistent across all tests, using the same GPC; the only variable was the volume of fibers incorporated, which varied at 0, 0.5, 0.75, and 1%. GPC samples enhanced with steel fibers demonstrated greater compressive strength in cube form when compared to those made without fiber reinforcement. The compressive strength increased by 21, 35. and 59% for the mixes H31, H41, and H51, corresponding to steel fiber amounts of 0.5, 0.75, and 1.0%, respectively. The inclusion of steel fibers enhanced the compressive strength, with the highest recorded magnitude being 59 MPa at 1.0% fiber amount. This result closely mirrors the conclusions of the study [25]. The lowest compressive strength among the fiberreinforced specimens was 40.5 MPa for mix H31, which still exceeded the 38.9 MPa observed in the GPC without steel fibers. Figure 7 illustrates the residual compressive strength of steel fiber-reinforced GPC mixtures subjected to high temps, compared to normal situations. The addition of steel fibers significantly improved strength retention under thermal subject. As fiber amount increased, the rate of strength degradation decreased, with higher fiber volumes demonstrating better thermal resistance and maintaining a greater portion of their original strength. At 250°C, an increase in residual strength was observed with increasing fiber volume, attributed to enhanced bonding between steel fibers and the geopolymer matrix due to continued polymerization microstructural densification. At normal temp, compressive strength rose from 38.9 MPa in the plain mix (H21) to 59 MPa in the 1.0% fiber mix (H51), a 52% improvement. Under high temps, fiber-reinforced mixes consistently outperformed the plain mix. At 750°C, H54 retained 27 MPa, more than double the 12.01 MPa of H24. Similar gains were noted at 250°C (from 30.1 MPa to 43.3 MPa) and 500°C (from 21.3 MPa to 32 MPa). These results confirm that increasing steel fiber amount enhances both normal and residual compressive strength, with 1.0% fiber providing the most effective improvement across all situations. The increase in compressive strength with steel fiber amount (0.5 to 1%) is due to the fibers' crack-bridging and reinforcement impact. Higher fiber volumes better restrict microcrack development, improve load transfer, and densify the matrix, leading to a regular and significant strength gain, while the base geopolymer mix remains the same.

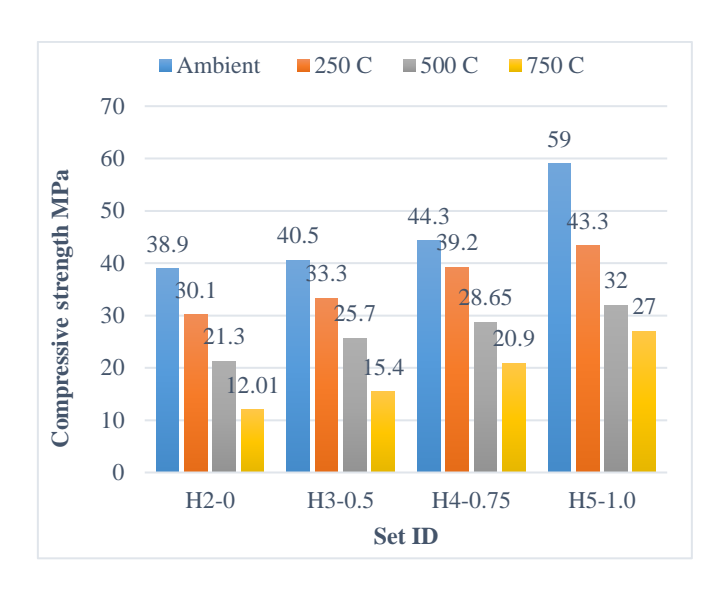
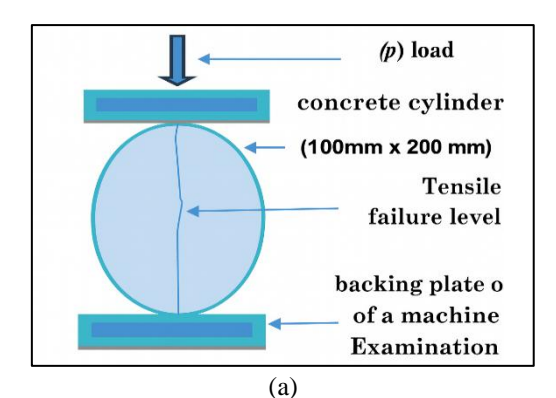


Figure 7. Compressive strength at different temps



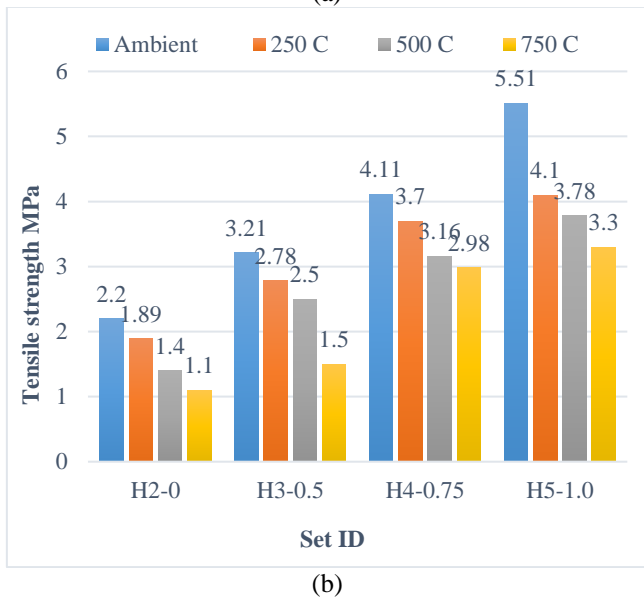


Figure 8. Tensile strength among different sets

(2) Specimens' tensile strength

Figure 8 shows the tensile strength was measured on cylindrical specimens with a diameter of 100 cm and a length of 20 cm, following ASTM C496 [26]. Residual strength tests were conducted on cylinders subjected to different fire intensities, subjected to fire temps of 250, 500, and 750°C. A total of 48 cylinders were tested, and the strength for each GPC mix is reported as the mean of three cylinders. All beams exhibited a reduction in tensile strength with increasing temp, mirroring the trend observed in compressive strength. For the

control specimens H22, H23, and H24 tensile strengths were 1.89, 1.4, and 1.1 MPa at 250, 500, and 750°C, corresponding to decreases of 14, 36, and 50%, respectively. With the addition of 0.5% steel fibers in samples (H32, H33, and H34), residual tensile strengths improved to 2.78, 2.5, and 1.5 MPa, with smaller reductions of 14, 22, and 53%. The samples H42, H43 and H44 showed further improvement, with tensile strength losses of only 10, 23, and 28%. Specimens H52, H53, H54 retained higher residual compressive strength, reaching up to 26, 31, and 40% at 250, 500, and 750°C, respectively. Overall, tensile strength declined as subject temp increased.

At 250°C, the tensile strength increased by 47%, 95%, and 117% for specimens H3 (0.5% SF), H4 (0.75% SF), and H5 (1.0% SF), respectively, compared to H2 (0% SF), following a trend similar to compressive strength. At 500°C, the residual tensile strengths were 1.4 MPa (H2), 2.5 MPa (H3), 3.16 MPa (H4), and 3.78 MPa (H5), reflecting increases of 79%, 125%, and 170% for fiber-reinforced mixes. This reduction in strength for H2 is attributed to partial decomposition and dehydration of calcium-aluminosilicate hydrate (C-A-S-H) due to limited water for chemical reactions. At 750°C, tensile strength continued to rise with increasing fiber amount: 1.1 MPa (H2), 1.5 MPa (H3), 2.98 MPa (H4), and 3.3 MPa (H5), marking gains of 36%, 170%, and 200% for H3, H4, and H5, respectively. The highest residual tensile strength (3.3 MPa) was achieved with 1.0% steel fiber, confirming the positive impact of fiber amount on thermal resistance. The tensile strength of GPC decreases with rising temp; however, adding steel fibers significantly improves its thermal resistance. At normal situations, strength increases with fiber amount, from 2.2 MPa (0% SF) to 5.51 MPa (1.0% SF). As the temp rises to 250, 500, and 750°C, all mixes show reduced strength, but fiber-reinforced specimens retain higher magnitudes. At 750°C, the 1.0% SF mix still achieves 3.3 MPa, compared to 1.1 MPa for the control. Overall, steel fibers enhance the residual tensile strength of GPC under high temps.

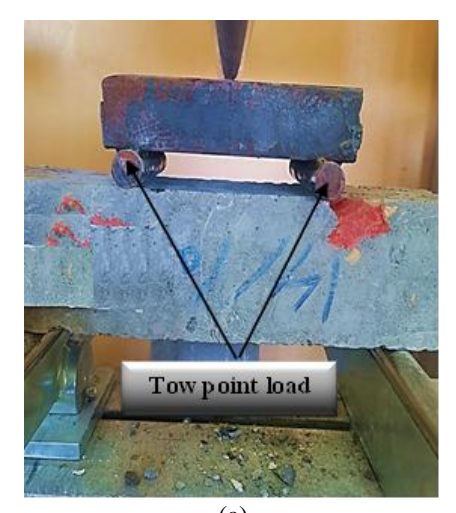
(3) Specimens' modulus of rupture

The modulus of rupture (f_r) of the GPC prismatic specimens was determined under normal situations and following subject to various fire intensities using a two-point load, in accordance with the reference [27], as illustrated in Figure 9. Prismatic specimens measuring $10 \times 10 \times 50$ cm were tested at 28 days of age. For each GPC mix, the reported strength represents the mean magnitude obtained from three specimens. Residual modulus of rupture tests was performed on prisms subjected to fire temps of 250, 500, and 750°C. In total, 48 prisms were tested, with the mean strength of three specimens reported for each mix. Figure 9 illustrates the impact of high temps on the flexural strength (modulus of rupture) of GPC specimens. An apparent decline in strength is observed as e temp increases across all steel fiber amount levels. For example, the modulus of rupture for the control specimen (H2-0%SF) decreases by 14% at 250°C compared to normal situations.

GPC specimens showed a significant reduction in flexural strength after fire subject, especially at 500 and 750°C. At 500°C, the residual flexural strength dropped to 66% for H2-0%SF and to 60%, 41%, and 38% for H3-0.5%SF, H4-0.75%SF, and H5-1%SF, respectively. At 750°C, the residual strength was 87% for H2-0%SF and 73%, 71%, and 69% for H3, H4, and H5. Despite the overall reduction, specimens with steel fibers (H3–H5) consistently outperformed the fiber-free mix (H2) across all fire subject levels. This aligns with observed gains in compressive and split tensile strengths.

Notably, H3-0.5%SF achieved flexural strengths of 5.14 MPa, 2.2 MPa, and 1.5 MPa at 250, 500, and 750°C, respectively. Compared to the plain GPC (G1-0%SF), H3 showed residual flexural strength improvements of 14%, 24%, and 117%, while H4 improved by 34%, 111%, and 168%, and H5 by 40%, 137%, and 204% at 250°C, 500°C, and 750°C, respectively.

The results clearly demonstrate that high temps significantly reduce the flexural strength (modulus of rupture) of all GPC specimens. However, the extent of strength loss varies depending on the steel fiber amount. The control mix without fibers (H2-0%) shows the most severe degradation, with the modulus of rupture decreasing from 5.25 MPa at normal temp to just 0.69 MPa at 750°C. In contrast, fiberreinforced mixes (H3-0.5%, H4-0.75%, and H5-1%) retain much higher residual strengths at all temps. Among these, H5-1%SF exhibits the best performance, maintaining a modulus of rupture of 2.1 MPa at 750°C—three times higher than the plain mix. This indicates that increasing steel fiber amount enhances the thermal resistance and structural integrity of GPC under fire subject. The positive influence of steel fibers is attributed to their crack-bridging ability and improved matrix cohesion, particularly at high temps. These findings confirm that steel fiber reinforcement is an effective strategy for improving the high-temp performance of GPC, making it more reliable for applications requiring enhanced fire resistance.



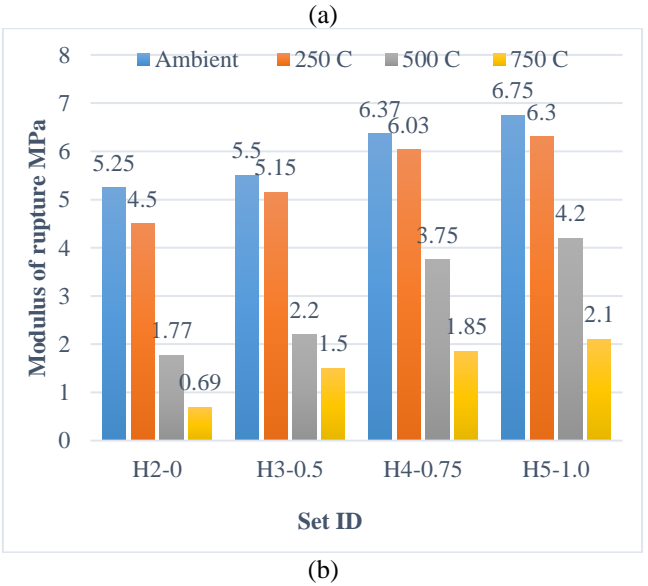


Figure 9. Flexural strength among different sets

3.2 Flexural response of reinforced GPC beams at ambient temperatures

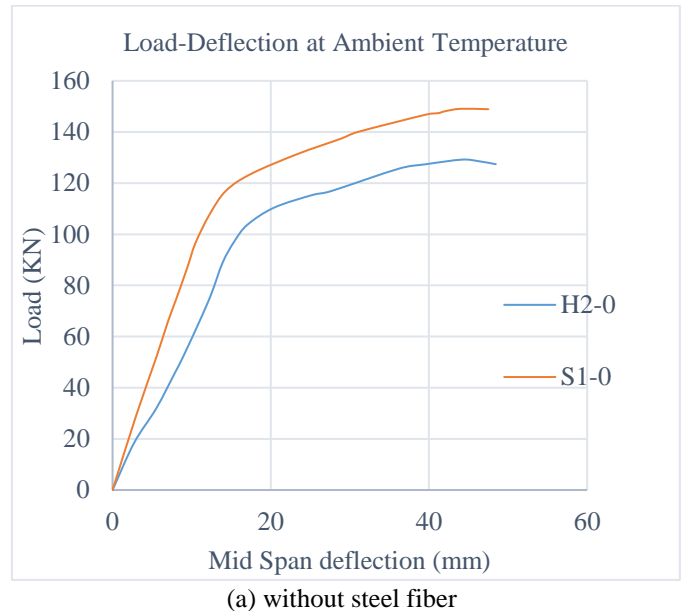
This section assesses the flexural behavior of both hollow and solid GPC beams, incorporating specimens with and without steel fibers. Mid-span deflections under flexural load were recorded using a Linear Variable Differential Transformer (LVDT). Table 5 summarizes the max loads (P_{u}) , maximum deflections (δ_{u}) , initial crack loads (P_{cr}) , and corresponding deflections.

Table 5. Crack and ultimate load vs. deflection results of GPC beams at ambient temperature

Beam Details	P _{cr} (kN)	Pu (kN)	Δcr (mm)	Δu (mm)
*S1-Am-0	29.3	152	2.1	42.2
**H2-Am-0	18.25	129	2.5	44.16
**H3-Am-0	23.56	138	2.9	52.4
**H4-Am-0	28.26	149	2.69	51.49
**H5-Am-0	41.46	161	2.53	50.85

^{*} Solid Section

^{**}Hollow Section



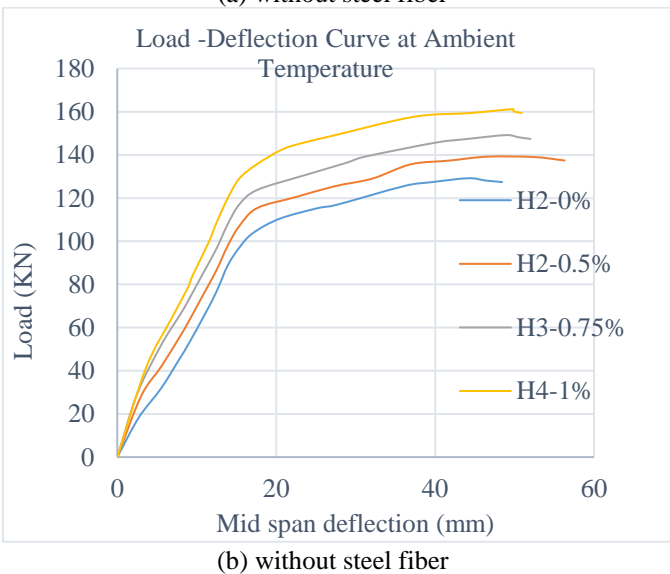


Figure 10. Load-deflection of solid and hollow beam

The cross-section type—hollow or solid—significantly affects beam performance. Solid beams generally have higher ultimate load capacities due to a larger cross-sectional area and better buckling resistance. As shown in Figure 10, the solid beam (S1-0%SF) carried 15% more load than the hollow beam (H2-0%SF). While hollow beams typically carry less load, they offer an efficient strength-to-weight ratio, making them

suitable for long spans or weight-sensitive structures, as shown in Figure 10(a).

The cross-section type—hollow or solid—significantly affects beam performance. Solid beams generally have higher max load capacities due to a larger cross-sectional area and better buckling resistance. As shown in Figure 10, the solid beam (S1) carried 15% more load than the hollow beam (H21). While hollow beams typically carry less load, they offer an efficient strength-to-weight proportion, making them suitable for long spans or weight-sensitive structures, as shown in Figure 10(a). Figure 10(b) presents the load-mid-span deflection responses of the tested hollow beams containing steel fibers, compared to the reference beam without fibers. The experimental data indicate that the max load capacities of beams H31, H41, and H51 increased by about 7, 16, and 25%, respectively, relative to the reference specimen H2-0%SF. The inclusion of steel fibers significantly improved the tensile performance of the GPC and limited crack propagation within the matrix. Moreover, the presence of fibers transformed the structural response of the beams, preventing sudden failure after the initiation of the first crack. Acting as crack-bridging elements, steel fibers enhanced the beams' ability to sustain loads beyond the cracking stage and contributed to improved ductility. Their role in redistributing internal stresses effectively inhibited crack growth under loading situations.

3.3 Ductility, stiffness, and toughness of hollow and solid beams

Ductility is a structure's capacity to endure significant deformation, especially in tension, without losing its load-bearing ability. It is determined by dividing the mid-span deflection at failure by the deflection at first yield of the tension reinforcement [28].

Ductility
$$=\frac{\delta_u}{\delta_v}$$
 (1)

As it is clear in Figure 11, solid beams generally exhibit higher ductility than hollow beams due to their continuous mass, enabling greater plastic deformation and energy absorption before failure. For instance, the ductility of solid beam S1 was about 6% higher than that of hollow beam H21, aligning with findings by Abdullah et al. [29]. Adding steel fibers further enhanced ductility—by about 10, 12, and 15% for H31, H41, and H51, respectively—due to the fibers' tensile strength and crack-bridging ability, which improve deformation capacity and reduce brittleness in GPC.

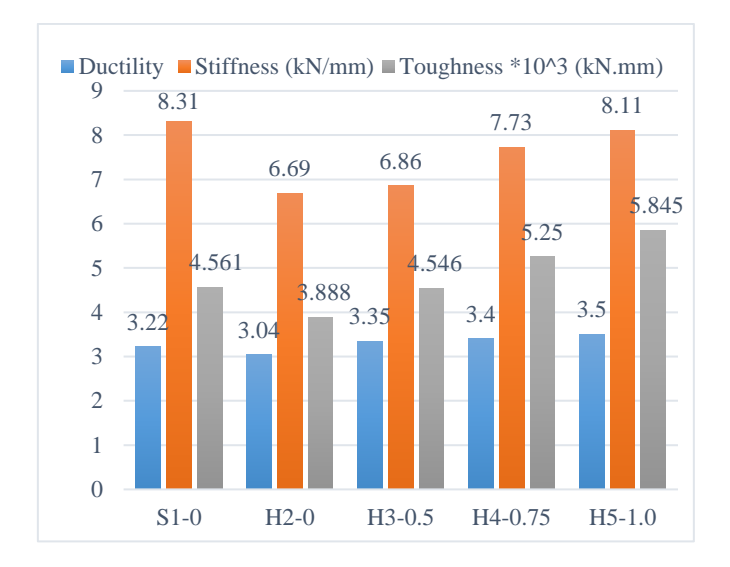


Figure 11. Flexural properties of solid and hollow beams under ambient temperature

Stiffness is a structural element's ability to resist deformation under load. The load is calculated by dividing it by the deflection, typically using 70% of the yield or max load [30]. On the other hand, the beam bending stiffness under force application could be analytically identified utilizing the beam deflection formula.

$$K = \frac{P_y}{\delta_y} \tag{2}$$

whereas,

K: the stiffness, P_y : the yield load, and δ_y : the deflection at the yield point.

As shown in Figure 11, the stiffness of the solid geopolymer beam (S1) was about 19% higher than that of the hollow beam (H21), due to the reduced material and strength in the hollow section. Adding steel fibers to hollow geopolymer beams increased stiffness by approximately 3, 16, and 21% for fiber amounts of 0.5, 0.75, and 1.0%, respectively, compared to the fiber-free hollow beam. The H51 beam exhibited the highest stiffness, as steel fibers enhance tensile stress transfer at cracks and better control of shrinkage cracks and strain [31]. Their high elastic modulus resists deformation and reduces crack width, thereby improving the beam's stiffness, especially under high loading by limiting crack propagation.

Flexural toughness is a beam's ability to absorb energy under loading before failure. It is quantified by the area under the load-deflection curve in a flexural test. As shown in Figure 11, the solid geopolymer beam (S1) had about 15% greater toughness than the hollow beam (H21), due to its higher material amount and better distribution of load. Adding steel fibers significantly improved the toughness of hollow beams, increasing it by 17%, 35%, and 50% for 0.5%, 0.75%, and 1.0% fiber amount, respectively. Steel fibers enhance energy absorption, crack resistance, and post-crack performance, improving the overall durability and resilience of GPC.

3.4 Structural effect of hollow and solid GPC beams under high temperature

This section examines the mid-span deflection of the beams subjected to three levels of fire subject: 250, 500, and 750°C, each under a sustained load equivalent to 50% of the beam's max capacity. The deflection corresponding to 50% of the max

load at normal temp is denoted as δ_a . After 120 minutes of fire subject, the resulting deflection is recorded as δ_β . The increase in deflection after 120 minutes, relative to δ_a , is also assessed.

(a) At 250°C

At 250°C, the mid-span deflections of S2 and H22 beams reached 16.2 mm and 19.8 mm, respectively. After 120 minutes, deflections increased by 93% for the solid beam (S2) and 128% for the hollow beam (H22), relative to their pre-fire magnitudes under 50% of max load. The solid beam (S2) showed about 22% lower deflection than the hollow beam, indicating better fire resistance. Hollow beams exhibit greater deflection under high temps than solid beams due to their internal voids, which reduce thermal resistance and increase vulnerability to bending. These voids may also house materials that degrade under heat, further contributing to deflection. In contrast, solid beams, with their higher density and structural integrity, offer better thermal resistance. As a result, at 250°C, hollow beams are likely to show more deflection than solid ones.

(b) At 500°C

Table 6 presents the impact of steel fiber (SF) amount on the mid-span deflection of GPC hollow beams subjected to 250°C under 50% of the max load. Deflections recorded after 2 hours were 19.8, 33.1, 28.6, and 26.9 mm for beams with 0, 0.5, 0.75, and 1% SF, respectively—corresponding to increases of 128%, 135%, 158%, and 110% over their pre-fire magnitudes. While the addition of SF enhances thermal resistance by stabilizing the matrix, reducing thermal expansion, and improving heat resistance, it also increases thermal conductivity, which can initially raise deflection. At 0.75% and 1% SF, performance improves, with 1% SF showing the lowest deflection increase, indicating the most effective thermal resistance at 250°C. At 500°C, mid-span deflection reached 21.8 mm for hollow beams and 18.7 mm for solid beams, confirming higher deflection in hollow sections. According to Table 7, deflections increased by 123% in S3 and 83% in H23 after 120 minutes compared to their initial magnitudes under service load. Solid beams demonstrated 17% lower deflection than hollow beams, indicating better resistance to heat-induced deformation. This improved performance is attributed to the solid structure's resistance to thermal shrinkage and mechanical degradation. Nonetheless, both beam types showed signs of thermal impacts, such as irregular expansion and shrinkage, due to changes in the geopolymer matrix at high temps.

Table 6. Deflection and increasing ratio of deflection for solid and hollow beam at 250°C

Beam Symbol	50% Load Pu	, .		Increasing (%)
	(kN)	Δa	Δb	(%)
S1-0%SF-250	76	8.4	16.2	93
H2-0%SF-250	65	8.7	19.8	128
H3-0.5% SF-250	69	14.1	33.1	135
H4-0.75% SF-250	75	11.1	28.6	158
H5-1.0%SF-250	81	12.8	26.9	110

(c) At 750°C

As shown in Table 7, the deflection behavior at 500°C differs from that observed at 250°C. After 2 hours of fire subject, mid-span deflections for beams H23, H33, H43, and H53 were 21.8 mm, 31.5 mm, 34.8 mm, and 35.9 mm,

respectively. Initial deflection was mainly driven by thermal bending due to non-uniform temp distribution across the beam thickness. After 120 minutes, deflection increases were recorded at 83%, 107%, 138%, and 153%, respectively. The inclusion of steel fibers led to a slight rise in deflection, with no significant improvement in performance. H23 showed the least increase in deflection, attributed to the superior thermal insulation features of the GPC matrix. At 750°C, the mid-span deflection of hollow beams (H23) reached 41.9 mm, while solid beams (S13) recorded 41.1 mm. Compared to deflection under service load, this represents an increase of 217% and 248% for H23 and S3, respectively, as shown in Table 8. Key factors influencing deflection under fire include the thermal conductivity of the mix and the effectiveness of bottom reinforcement. Despite the slight difference, solid beams showed better resistance, with 2% lower deflection than hollow beams under identical situations. Solid GPC beamsmaintained integrity for the full 120 minutes due to their high thermal stability, low chemically bound water, and resistance to spalling. Although some stiffness loss and surface cracking occurred due to thermal expansion, the cracks did not compromise structural integrity, owing to the inherent flexibility of GPC.

Table 7. Deflection and increasing ratio of deflection for solid and hollow beam at 500°C

Beam Symbol	50% Load Pu	Defle (m	ction m)	Increasing (%)
	(kN)	Δa	Δb	(/0)
S1-0%SF-500	76	8.4	18.7	123
H2-0%SF-500	65	11.9	21.8	83
H3-0.5%SF-500	69	15.2	31.5	107
H4-0.75%SF-500	75	14.6	34.8	138
H5-1.0%SF-500	81	14.2	35.9	153

Table 8. Deflection and increasing ratio of deflection for solid and hollow beam at 750°C

Beam Symbol	50% Load Pu		ection nm)	Increasing (%)
	(kN)	Δa	Δb	(%)
S1-0%SF-750	76	11.8	41.1	248
H2-0%SF-750	65	13.2	41.9	217
H3-0.5%SF-750	69	16.3	44.8	175
H4-0.75%SF-750	75	15.8	46.9	197
H5-1.0%SF-750	81	15.3	48.5	217

According to the study [32], at 750°C—the most critical fire subject level tested-all GPC beams exhibited increased midspan deflection and deflection rates. Deflections continued to rise until failure, with significant increases noted from the beginning of the test. Audible cracking and popping sounds were detected after 60 minutes, attributed to thermal stress. Hollow beams without steel fibers (H24) failed earliest, around 70 minutes, while those with steel fibers (H3-H5) resisted longer, failing between 80-100 minutes, as shown in Table 8. Steel fibers enhanced the structural fire resistance and delayed collapse. Post-failure deflections were 41.9 mm (H24), 44.8 mm (H34), 46.9 mm (H44), and 48.5 mm (H54). Despite this, H24 showed the lowest deflection, likely due to its lower thermal conductivity, which slowed heat penetration and delayed reinforcement degradation. The deflection increases, relative to the service load, were 217% (H24), 175% (H34), 197% (H4), and 217% (H54). The most influential factors on deflection were the mix's thermal conductivity and the presence of bottom reinforcement. Although steel fibers improved fire endurance, they did not significantly reduce deflection, as deflection trends remained similar across SF-reinforced beams.

3.5 Residual strength after fire

Residual strength refers to the remaining load-bearing capacity of a material after fire subject. It is influenced by factors such as material type, temp level, subject duration, and cooling method. To assess this, the same flexural test used on unsubjected beams was applied post-fire. For solid beams, residual strengths at 250 and 500°C were about 12 and 25%, respectively (Table 9). While the impact at 250°C was minor, strength loss became more significant at 500°C. Solid beams performed better than hollow beams due to their greater mass, which promotes even heat distribution and reduces thermal stress. In contrast, hollow sections are more prone to early cracking from temp gradients.

Table 9. Residual strength after exposure to fire

Symbol	Temp.	Ultimate Load (kN)	Residual Load (kN)	Decreasing (%)
S1-0% SF- 250		152	134	12
H2-0% SF- 250		129	106	18
H3-0.5% SF-250	250°C	138	110	20
H4-0.75% SF-250		149	117	21
H5-1.0% SF-250		161	130	19
S1-0% SF- 500		152	109	24
H2-0% SF- 500		129	96	26
H3-0.5% SF-500	500°C	138	101	27
H4-0.75% SF-500		149	104	30
H5-1.0% SF-500		161	121	25
S1-0% SF- 750	750°C	152	87	47

At 250°C, the residual strengths of hollow beams H22, H32, H42, and H52 were 18, 20, 21, and 19%, respectively. Steel fibers contributed to maintaining strength under heat. At 500°C, these magnitudes dropped to 26, 27, 30, and 25%, showing that fiber-reinforced GPC can still carry loads at high temps. At 750°C, all hollow beams failed. However, solid beams retained about 47% of their strength after two hours of subject, confirming their superior post-fire performance. GPC, characterized by its aluminosilicate-based composition rather than traditional calcium silicates, exhibits enhanced resistance to heat and fire. Its chemical structure provides superior thermal stability and lowers the risk of spalling. However, due to retained moisture within the matrix, GPC may undergo explosive spalling at temps exceeding 500°C, leading to the sudden loss of surface layers.

4. CONCLUSION

The incorporation of steel fibers significantly enhances the

mechanical and thermal performance of GPC, with a 1.0% steel fiber (SF) amount yielding the highest improvements in compressive, tensile, and flexural strengths under both normal and high temp situations. Solid GPC beams consistently outperform their hollow counterparts, demonstrating up to 18% higher load-bearing capacity, alongside superior stiffness, ductility, toughness, and enhanced fire resistance. In hollow GPC beams, the addition of steel fibers improves structural stiffness, deformation capacity, and resistance to crack propagation, with optimal performance observed at 1.0% SF. During fire subject, fiber-reinforced hollow beams initially experienced increased mid-span deflection, which stabilizes after 120 minutes, particularly at the 1.0% SF dosage. Post-fire testing reveals that solid GPC beams undergo significantly less deflection than hollow beams, reflecting greater resistance to thermal-induced deformation. Moreover, solid beams retain up to 47% of their original load-carrying capacity at 750°C due to increased mass and thermal inertia, offering superior residual strength relative to hollow sections. While hollow beams reinforced with steel fibers maintain structural integrity up to 500°C, all specimens failed at 750°C. Steel fibers further contribute to thermal resistance by enhancing compressive and tensile strengths and mitigating spalling through the regulation of internal vapor pressures. Both solid and hollow GPC beams retain substantial mechanical capacity after subject to 250°C, with negligible degradation. However, at 500°C, a noticeable reduction in residual strength is observed, though fiber inclusion mitigates this loss. At 750°C, all hollow beams experience structural failure, whereas solid beams exhibit marked flexural strength degradation relative to normal situations.

5. LIMITATIONS AND FUTURE WORK

This study deliberately focused on the thermo-mechanical response of full-scale structural elements, specifically solid and hollow geopolymer concrete beams reinforced with steel fibers. No microstructural tests such as SEM, XRD, or TGA were performed, as the objective was to evaluate beam-level performance under elevated temperatures. Future investigations should incorporate microstructural analyses to correlate phase transformations, pore evolution, and fiber—matrix interactions with the observed flexural and residual strength behavior. Such integration would provide a more comprehensive understanding of the micro—macro linkage governing fire resistance in geopolymer structural systems.

REFERENCES

- [1] Sharma, U., Gupta, N., Bahrami, A., Özkılıç, Y.O., Verma, M., Berwal, P., Althaqafi, E., Khan, M.A., Islam, S. (2024). Behavior of fibers in geopolymer concrete: A comprehensive review. Buildings, 14(1): 136. https://doi.org/10.3390/buildings14010136
- [2] Al-Husseinawi, F.N., Atherton, W., Al-Khafaji, Z., Sadique, M., Yaseen, Z.M. (2022). The impact of molar proportion of sodium hydroxide and water amount on the compressive strength of slag/metakaolin (waste materials) geopolymer mortar. Advances in Civil Engineering, 2022(1): 5910701. https://doi.org/10.1155/2022/5910701
- [3] Mohammed, Z.A., Al-Jaberi, L.A., Shubber, A.N.

- (2021). Polypropylene fibers reinforced geopolymer concrete beams under static loading, part 1: Underreinforced section. AIP Conference Proceedings, 2372(1): 180010. https://doi.org/10.1063/5.0065392
- [4] Zeini, H.A., Al-Jeznawi, D., Imran, H., Bernardo, L.F.A., Al-Khafaji, Z., Ostrowski, K.A. (2023). Random forest algorithm for the strength prediction of geopolymer stabilized clayey soil. Sustainability, 15(2): 1408. https://doi.org/10.3390/su15021408
- [5] AL-JABERI, L.A., Ali, A., Al-Jadiri, R.S., Al-Khafaji, Z. (2023). Workability and compressive strength properties of (fly ash-metakaolin) based flowable geopolymer mortar. Electronic Journal of Structural Engineering, 23(4): 46-51. https://doi.org/10.56748/ejse.23436
- [6] Figiela, B., Šimonová, H., Korniejenko, K. (2022). State of the art, challenges, and emerging trends: Geopolymer composite reinforced by dispersed steel fibers. Reviews on Advanced Materials Science, 61(1): 1-15. https://doi.org/10.1515/rams-2021-0067
- [7] Falah, M., Al-Khafaji, Z. (2022). Behaviour of reactive powder concrete hollow core columns strengthened with carbon fiber reinforced polymer under eccentric loading. Electronic Journal of Structural Engineering, 22(3): 28-38. https://doi.org/10.56748/ejse.223293
- [8] Lateef, H.A., Alabdulhady, M.Y., Naser, K.Z. (2025). A comprehensive evaluation of concrete behavior made with date seed as a partial replacement of fine aggregate. Mathematical Modelling of Engineering Problems, 12(6): 2097-2109. https://doi.org/10.18280/mmep.120625
- [9] Hamoodi, A.Z., Alhussein, T.H., Zewair, M.S., Naser, K.Z. (2025). Experimental study for the effect of steel fibers types and volume fraction on the flexural performance of RC beams. Mathematical Modelling of Engineering Problems, 12(7): 2203-2215. https://doi.org/10.18280/mmep.120701
- [10] Madheswaran, C.K., Gnanasundar, G., Gopalakrishnan, N. (2013). Effect of molarity in geopolymer concrete. International Journal of Civil & Structural Engineering, 4(2): 106-115.
- [11] Arun, B.R., Nagaraja, P.S., Mahalingasharma, S. (2018). Combined effect of flyash & GGBS on workability and mechanical properties of self compacting geopolymer concrete. International Journal of Pure and Applied Mathematics, 119(15): 1369-1380.
- [12] Majdi, H.S., Shubbar, A.A., Nasr, M.S., Al-Khafaji, Z.S., Jafer, H., Abdulredha, M., Al Masoodi, Z., Sadique, M., Hashim, K. (2020). Experimental data on compressive strength and ultrasonic pulse velocity properties of sustainable mortar made with high content of GGBFS and CKD combinations. Data in Brief, 31: 105961. https://doi.org/10.1016/j.dib.2020.105961
- [13] Abdullah, A.F., Ezuldin, N.Y., Ahmed, I.M., Al-Khafaji, Z. (2025). Enhancing the sustainability of concrete mixes utilizing supplementary cementitious materials in renewable energy buildings. Engineering, Technology & Applied Science Research, 15(5): 28041-28049. https://doi.org/10.48084/etasr.12936
- [14] Al-Bayati, M.A., Abdulrahman, M.B., Alzeebaree, R., Arbili, M.M. (2022). The effect of materials and curing system on the behavior of self-compacting geopolymer concrete. Journal of the Mechanical Behavior of Materials, 31(1): 710-718.

- https://doi.org/10.1515/jmbm-2022-0206
- [15] Bellum, R.R., Nerella, R., Madduru, S.R.C., Indukuri, C.S.R. (2019). Mix design and mechanical properties of fly ash and GGBFS-synthesized alkali-activated concrete (AAC). Infrastructures, 4(2): 20. https://doi.org/10.3390/infrastructures4020020
- [16] Saavedra, W.G.V., de Gutiérrez, R.M. (2017). Performance of geopolymer concrete composed of fly ash after exposure to elevated temperatures. Construction and Building Materials, 154: 229-235. https://doi.org/10.1016/j.conbuildmat.2017.07.208
- [17] Behfarnia, K., Shahbaz, M. (2018). The effect of elevated temperature on the residual tensile strength and physical properties of the alkali-activated slag concrete. Journal of Building Engineering, 20: 442-454. https://doi.org/10.1016/j.jobe.2018.08.015
- [18] Abdullah, A.F., Abdul-Rahman, M.B.A.D., Al-Attar, A.A. (2024). A review on geopolymer concrete behaviour under elevated temperature influence. Journal of Sustainability Science and Management, 19(12): 239-259. https://doi.org/10.46754/jssm.2024.12.014
- [19] Ahmed, L.A.Q. (2023). Durability of normal and light weight geo polymer concrete exposed to elevated temperature. PhD thesis, University of Technology.
- [20] ACI Committee 233. (2003). 233R-03: Slag Cement in Concrete and Mortar. https://www.concrete.org/store/productdetail.aspx?Item ID=23303&Format=DOWNLOAD&Language=English &Units=US Units.
- [21] ASTM C618-22. (2023). Standard specification for coal fly ash and raw or calcined natural pozzolan for use in concrete. ASTM Standards. https://doi.org/10.1520/C0618-22
- [22] Republic of Iraq Ministry of Planning. (2022). Central Organization for Standardization and Quality Control. https://mop.gov.iq/en/central-organization-for-standardization-and-quality-control.
- [23] Aggregate from natural sources for concrete IQ.S 45/1984. In Iraqi Standard (Materials Specification & Construction Works), 2004. https://www.scribd.com/document/395467049/Iraqi-Standard-Materials-Specification-Construction-Works.

- [24] Me, C.R., Rao, A.B. (2014). Behavior of self compacting concrete under axial compression with and without confinement. International Journal of Ethics in Engineering & Management Education, 1(3): 8-16.
- [25] Abdul-Rahman, M.B., Al-attar, A.A., Younus, A.M. (2018). Elevated temperature effects on the behavior of one-way fibrous reinforced concrete slabs. International Journal of Engineering & Technology, 7(437): 179-184. https://doi.org/10.14419/ijet.v7i4.37.24097
- [26] ASTM C496-96. (2008). Standard test method for splitting tensile strength of cylindrical concrete specimens. ASTM Standards. https://doi.org/10.1520/C0496-96
- [27] Test, C.C., Drilled, T. (2010). Standard test method for flexural strength of concrete (using simple beam with third-point loading) 1. Hand, 78(C): 1-4.
- [28] Elsayed, M., Tayeh, B.A., Aisheh, Y.I.A., Abd El-Nasser, N., Abou Elmaaty, M. (2022). Shear strength of eco-friendly self-compacting concrete beams containing ground granulated blast furnace slag and fly ash as cement replacement. Case Studies in Construction Materials, 17: e01354. https://doi.org/10.1016/j.cscm.2022.e01354
- [29] Abdullah, A.F., Abdul-Rahman, M.B.A.D., Al-Attar, A.A. (2025). Investigate the mechanical characteristics and microstructure of fibrous-geopolymer concrete exposure to high temperatures. Journal of Rehabilitation in Civil Engineering, 14(1): 2141. https://doi.org/10.22075/jrce.2025.34716.2141
- [30] Hason, M.M., Hanoon, A.N., Saleem, S.J., Hejazi, F., Al Zand, A.W. (2021). Characteristics of experimental ductility energy index of hybrid-CFRP reinforced concrete deep beams. SN Applied Sciences, 3(2): 200. https://doi.org/10.1007/s42452-021-04202-6
- [31] Gomes, R.F., Dias, D.P., de Andrade Silva, F. (2020).

 Determination of the fracture parameters of steel fiberreinforced geopolymer concrete. Theoretical and
 Applied Fracture Mechanics, 107: 102568.
 https://doi.org/10.1016/j.tafmec.2020.102568
- [32] ASTM E119-20. (2023). Standard Test Methods for Fire Tests of Building Construction and Materials. ASTM Standards. https://doi.org/10.1520/E0119-20